Drug Design, Development and Therapy

Dovepress
open access to scientific and medical research

Open Access Full Text Article

ORIGINAL RESEARCH

Liquiritin Protects Against Cardiac Fibrosis After Myocardial Infarction by Inhibiting CCL5 Expression and the NF-κB Signaling Pathway

Xue Han[1,*], Yakun Yang[1,*], Muqing Zhang[2,3], Li Li[4], Yucong Xue[2], Qingzhong Jia[4], Xiangting Wang[2,5], Shengjiang Guan[3,6]

[1]School of Pharmacy, Hebei University of Chinese Medicine, Shijiazhuang, People's Republic of China; [2]College of Integrative Medicine, Hebei University of Chinese Medicine, Shijiazhuang, People's Republic of China; [3]Affiliated Hospital, Hebei University of Chinese Medicine, Shijiazhuang, People's Republic of China; [4]School of Pharmacy, Hebei Medical University, Shijiazhuang, People's Republic of China; [5]Hebei Key Laboratory of Integrative Medicine on Liver-Kidney Patterns, Shijiazhuang, People's Republic of China; [6]School of Basic Medicine, Hebei University of Chinese Medicine, Shijiazhuang, People's Republic of China

*These authors contributed equally to this work

Correspondence: Xiangting Wang, College of Integrative Medicine, Hebei University of Chinese Medicine, Shijiazhuang, Hebei, People's Republic of China, Email wangxiangting@hebcm.edu.cn; Shengjiang Guan, Affiliated Hospital, Hebei University of Chinese Medicine, Shijiazhuang, Hebei, People's Republic of China, Email guanshengjiang123@126.com

Purpose: Despite significant advances in interventional treatment, myocardial infarction (MI) and subsequent cardiac fibrosis remain major causes of high mortality worldwide. Liquiritin (LQ) is a flavonoid extract from licorice that possesses a variety of pharmacological properties. However, to our knowledge, the effects of LQ on myocardial fibrosis after MI have not been reported in detail. The aim of our research was to explore the potential role and mechanism of LQ in MI-induced myocardial damage.

Methods: The MI models were established by ligating the left anterior descending branch of the coronary artery. Next, rats were orally administered LQ once a day for 14 days. Biochemical assays, histopathological observations, ELISA, and Western blotting analyses were then conducted.

Results: LQ improved the heart appearance and ECG, decreased cardiac weight index and reduced levels of cardiac-specific markers such as CK, CK-MB, LDH, cTnI and BNP. Meanwhile, LQ reduced myocardial infarct size and improved hemodynamic parameters such as LVEDP, LVSP and $\pm dp/dt_{max}$. Moreover, H&E staining showed that LQ attenuated the pathological damage caused by MI. Masson staining showed that LQ alleviated myocardial cell disorder and fibrosis while reducing collagen deposition. LQ also decreased the levels of oxidative stress and inflammation. Western blotting demonstrated that LQ significantly down-regulated the expressions of Collagen I, Collagen III, TGF-β1, MMP-9, α-SMA, CCL5, and p-NF-κB.

Conclusion: LQ protected against myocardial fibrosis following MI by improving cardiac function, and attenuating oxidative damage and inflammatory response, which may be associated with inhibition of CCL5 expression and the NF-κB pathway.

Keywords: liquiritin, cardiac fibrosis, myocardial infarction, CCL5 expression, NF-κB signaling pathway

Introduction

Timely and complete myocardial reperfusion (eg, thrombolytic therapy or primary percutaneous coronary intervention) is an effective treatment to reduce ischemic injury and infarct size, but myocardial fibrosis (MF) after myocardial infarction (MI) still leads to adverse cardiac remodeling and high mortality.[1,2] Fibrosis represents one of the primary mechanisms involved in the repair process after MI, which may manifest as interstitial and replacement fibrosis.[3,4] MF is an irreversible structural change of the heart caused by excessive deposition of extracellular matrix (ECM).[5] Collagen I (50–85%) and collagen III (10–45%) are the major collagens in the myocardial ECM.[6] Myofibroblasts express α-smooth muscle actin (α-SMA) and coordinate deposition of collagen and secretion of multiple ECM proteins.[7] Matrix metalloproteinases (MMPs) are known regulators of cardiac remodeling.[8] All kinds of cytokines, inflammatory factors,

Received: 19 August 2022
Accepted: 28 November 2022
Published: 2 December 2022

and the oxidative stress may promote fibroblast proliferation and synthesis of large amounts of collagen, leading to MF.[9–11]

It is well known that the inflammatory response could further aggravate the cardiac remodeling and myocardial damage.[12] C-C chemokine motif ligand 5 (CCL5) is a typical pro-inflammatory chemokine. CCL5 is also named regulated on activation normal T cell expressed and secreted (RANTES).[13] During various pathological processes, CCL5 enhances and directs leukocyte migration to inflammatory response lesions.[14,15] CCL5 is expressed in a variety of cells and could activate the downstream pathway of nuclear factor kappa-B (NF-κB) by binding to surface receptors.[16] It has been reported that CCL5 expression is increased in myocardial reperfusion injury.[14]

The NF-κB pathway has long been considered as a typical pro-inflammatory signaling pathway. This is based primarily on the function of NF-κB in the expression of pro-inflammatory genes, which include chemokines, cytokines, and adhesion molecules.[17] Activation of NF-κB after MI and its subsequent nuclear translocation trigger the transcription of a large number of pro-inflammatory genes, which further amplifies the inflammatory response and damages cardiomyocytes.[18] Therefore, drugs that selectively treat injurious fibrosis and pro-inflammatory signals could help to reduce the incidence of MI.

In recent years, licorice (gancao in Chinese) has attracted much attention due to its rich phytochemical composition and the application of compounded formulations.[19] Liquiritin (LQ, Figure 1) is a flavonoid extract from licorice that possesses a variety of pharmacological properties, such as antidepressant, anti-inflammatory, antitumor, and cardiovascular protection properties.[20] Recent studies have reported that LQ exerts cardioprotective effects by attenuating oxidative stress injury, reducing the expression of inflammatory factors, inhibiting cell apoptosis, restoring cardiac functional parameters and maintaining structural integrity.[21–23] In addition, many traditional Chinese medicine formula containing LQ have been used to treat cardiovascular diseases, especially ischemic heart disease, such as Zhigancao Decoction,[24] Xuefu Zhuyu Decoction,[25] Yangxin Dingji Capsule,[26] etc. However, the effect of LQ on MI-induced damage remains poorly understood. This study was designed to test the hypothesis that LQ exhibits cardioprotective effects by attenuating MF and inhibiting related pathways in a rat model of MI.

Materials and Methods

Reagents

LQ was supplied by Chengdu Alfa Biotechnology Co., Ltd. (Chengdu, China). The primary antibodies of anti-Collagen I (catalog: WL0088), anti-Collagen III (catalog: WL03186), anti-TGF-β1 (catalog: WL02193), anti-MMP-9 (catalog: WL03096), anti-α-SMA (catalog: WL02510), anti-NF-κB (catalog: WL01980), anti-p-NF-κB (catalog: WL02169), and anti-β-actin (catalog: WL01372) were provided by Wanleibio Biotechnology Co., Ltd. (Shenyang, China). The primary antibodies of anti-CCL5 (catalog: A14192) were obtained from ABclonal Technology Co., Ltd. (Wuhan, China). Except where otherwise specified, all additional analysis-grade reagents for this study were provided by the Sigma Chemical Company (MO, USA).

Experimental Animals

All experiments were performed using adult male Sprague-Dawley (SD) rats, weighing between 200 and 250 g (6–8 weeks old), which were provided by Liaoning Changsheng Biotechnology Co., Ltd. (SCXK 2020–0001). The rats were

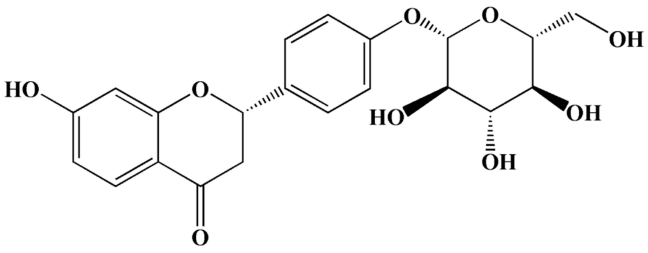

Figure 1 Chemical structure of LQ.

kept in 12-h light/dark cycles with unrestricted access to food and water at a constant room temperature of 23°C ± 1°C. Every attempt was made to reduce the number of animals utilized and their suffering. Our animal experimental procedures were reviewed and approved by the Animal Ethics Committee of Hebei University of Traditional Chinese Medicine (DWLL2018003) and were in accordance with the National Institutes guidelines for the Care and Use of Laboratory Animals.

Establishment of MI Model

Anesthesia was established with sodium pentobarbital (40 mg/kg) via intraperitoneal injection, and then the rats were immobilized and connected to a heart monitor and HX101E small animal ventilator (Chengdu TECHMAN, China). We bluntly detached the thoracic muscles, rapidly extruded the heart, and ligated the left anterior descending branch of the coronary artery. Myocardial bleaching and ST-segment elevation on the electrocardiogram indicated that the model was successfully established.[27–29] The sham-operated group was operated on identically except that the coronary artery was not ligated. The animals were carefully monitored during the establishment of the model.

All rats were randomly divided into six groups consisting of seven rats each: 1) sham-operated rats (Sham), 2) MI rats (MI), 3) MI rats given 20 mg/kg LQ (MI+L-LQ), 4) MI rats given 40 mg/kg LQ (MI+M-LQ), 5) MI rats given 80 mg/kg LQ (MI+H-LQ),[30–32] and 6) MI rats given 6 mg/kg verapamil (MI+VER). Finally, rats were injected intraperitoneally with 40 mg/kg sodium pentobarbital for anesthesia.

Determination of Electrocardiogram (ECG) and Cardiac Weight Index (HW/BW)

The BL420S physiological experiment system (Chengdu TECHMAN, China) was used to record the typical ECG trajectory of the rat heart. The right upper limb, right lower limb, and left lower limb of the rat were connected with white, red, and black subcutaneous needle electrodes, respectively. The rats were sacrificed, and then blood was carefully collected while taking care to prevent hemolysis. The hearts were removed within minutes, rinsed with saline, weighed, and photographed. HW/BW was calculated as the ratio of the heart mass (mg) to the total body mass (g). The heart tissues were collected, partially frozen in liquid nitrogen, and partially fixed in 10% neutral buffered formalin for further analysis.

Detection of Released CK, LDH, CK-MB, cTnI and BNP

Serum was separated from the collected whole blood by centrifugation (1301 g for 10 min), and assay kits were used to detect CK (JianCheng, Nanjing, China, catalog: A032) and LDH (Wanleibio, Shenyang, China, catalog: WLA072). The content of CK-MB (JianCheng, Nanjing, China, catalog: H197-1-1), cTnI (Wuhan Fine Biotech Co., Ltd., Wuhan, China, catalog: P2477) and BNP (Wuhan Fine Biotech Co., Ltd., Wuhan, China, catalog: EH2718) were assessed by enzyme-linked immunosorbent assay (ELISA). The activity of CK was calculated based on the amount of inorganic phosphorus produced. Similarly, the amount of LDH was assessed by measuring the level of pyruvate. The absorbance was measured at 660 nm and 450 nm for CK and LDH, respectively.[33] Absorbance was analyzed by using an UV752N Ultraviolet Spectrophotometer (Youke, Shanghai, China).

Detection of Myocardial Infarct Size and Hemodynamics

The ischemic myocardium was stained with tetrazolium chloride (TTC) to visualize its macroscopic morphology. Briefly, hearts were placed at −80°C for 20 min, cut transversely into 5 slices from the apices, and then incubated at 37°C for 5–8 min with 0.4% TTC solution. During this process, the sections were turned over once or twice so that they were immersed in and covered by the solution. Finally, the heart sections were placed in normal saline and photographed with a camera. Computer software (Image-Pro Plus version 6.0) was then used to calculate the proportion of the infarct area to the total myocardial tissue area (%).

A polyethylene tube with an outer diameter of 0.90 mm and an inner diameter of 0.50 mm was inserted into the left ventricle through the right carotid artery. A PowerLab 8/30 instrument (ADInstruments, Australia) was used to measure the left ventricular end-diastolic pressure (LVEDP) and left ventricular systolic pressure (LVSP). Using the continuously collected pressure sign, we calculated the highest rate of pressure contraction ($+dP/dt_{max}$) and its lowest rate of relaxation ($-dP/dt_{max}$).[23]

Detection of H&E and Masson Staining

For each group, the hearts were fixed in 10% neutral formalin for 48 h, dehydrated, hyalinized, macerated, and embedded in paraffin. Next, samples were cut into 5-mm-thick layers, and staining with hematoxylin and eosin (H&E) and Masson kits was performed. Almost all areas of the three sections in each group were observed with a BX53 microscope (Olympus, Japan), and representative images were captured with a DP73 camera system (Olympus, Japan). Image-Pro Plus version 6.0 was used to quantify positive signals of myocardial injury. Then, the percentage of positive areas for H&E and Masson staining were calculated.

Detection of SOD and MDA

Kits for SOD and MDA were provided by Wanlei Biotechnology Co., Ltd. (Shenyang, China). Biochemical parameters SOD (catalog: WLA110) and MDA (catalog: WLA048) were analyzed using a biochemical analyzer, and all steps were completed according to the instructions provided with the kit. The SOD assay is based on the xanthine and xanthine oxidase reaction system to produce superoxide anion radicals. The latter then oxidizes hydroxylamine to form nitrite, which appears purplish-red in the presence of a chromogenic agent. Finally, the absorbance is measured at 550 nm. Under acidic and high temperature conditions, MDA can react with thiobarbituric acid (TBA) to form a reddish-brown product. The absorbance was measured at its maximum absorption wavelength of 532 nm.[34]

Detection of Inflammatory Cytokines

The heart tissue samples were accurately weighed, and 9 times the volume (ie, 9 mL per 1 g) of homogenized medium (0.9% saline) was added to prepare a 10% homogenate. The analysis of inflammatory factors was performed by sandwich Enzyme-linked immunosorbent assay (ELISA). The levels of IL-6 (Wanleibio Biotechnology Co., Ltd. Shenyang, China, 1:50, catalog: WLE04) and TNF-α (Wanleibio Biotechnology Co., Ltd. Shenyang, China, 1:50, catalog: WLE05) were determined from the supernatant. The process was strictly based on the manufacturer's instructions.

Western Blot Analysis

A total of 40 μg of proteins were separated using 8–15% SDS-PAGE and transferred onto PVDF membranes (0.45 μm; Millipore, USA). The PVDF membranes were cut according to the molecular weight before antibody incubation. Incubation of the membranes was carried out with TBST for 5 min, followed by sealing with sealing buffer (5% milk) for 1 h at 37°C. Next, the transferred membranes were blotted with antibodies overnight at 4°C with primary antibodies against Collagen I (1: 500, dilution), Collagen III (1: 500, dilution), TGF-β1(1: 500, dilution), MMP-9 (1: 500, dilution), α-SMA (1: 500, dilution), CCL5 (1: 1000, dilution), NF-κB (1: 500, dilution), p-NF-κB (1: 500, dilution), and β-actin (1: 1000, dilution). The membrane was then washed three times with TBST and incubated for 45 min at 37°C with the corresponding secondary antibody. The protein blots were visualized with an ECL kit (Wanleibio Biotechnology Co., Ltd. Shenyang, China, catalog: WLA003) and then developed on the X-ray film in a dark room. Finally, chemiluminescent darkroom development was used to scan and acquire images, and optical density values of target bands were analyzed using a Gel-Pro-Analyzer system. The results were analyzed to calculate the optical density ratio of the target protein to the internal β-actin band.

Statistical Analysis

All quantitative data were expressed as the mean ± SEM and analyzed by Origin Pro version 9.1 software. Data were examined for normality of the distribution by the Shapiro–Wilk test prior to statistical analysis. Statistical significances of multiple-group were examined using ANOVA with a post-hoc Tukey's test (normally distributed) or Kruskal–Wallis with a post-hoc Dunn's test (nonnormally distributed). P values < 0.05 indicated statistical significance.

Results

LQ Improved Gross Appearances, ECG, and HW/BW

As shown in Figure 2A, the gross appearance of the heart shows that MI causes an enlarged heart that appears brown and swollen. However, the heart pathology dramatically improved with both LQ and VER, and the hearts resembled those

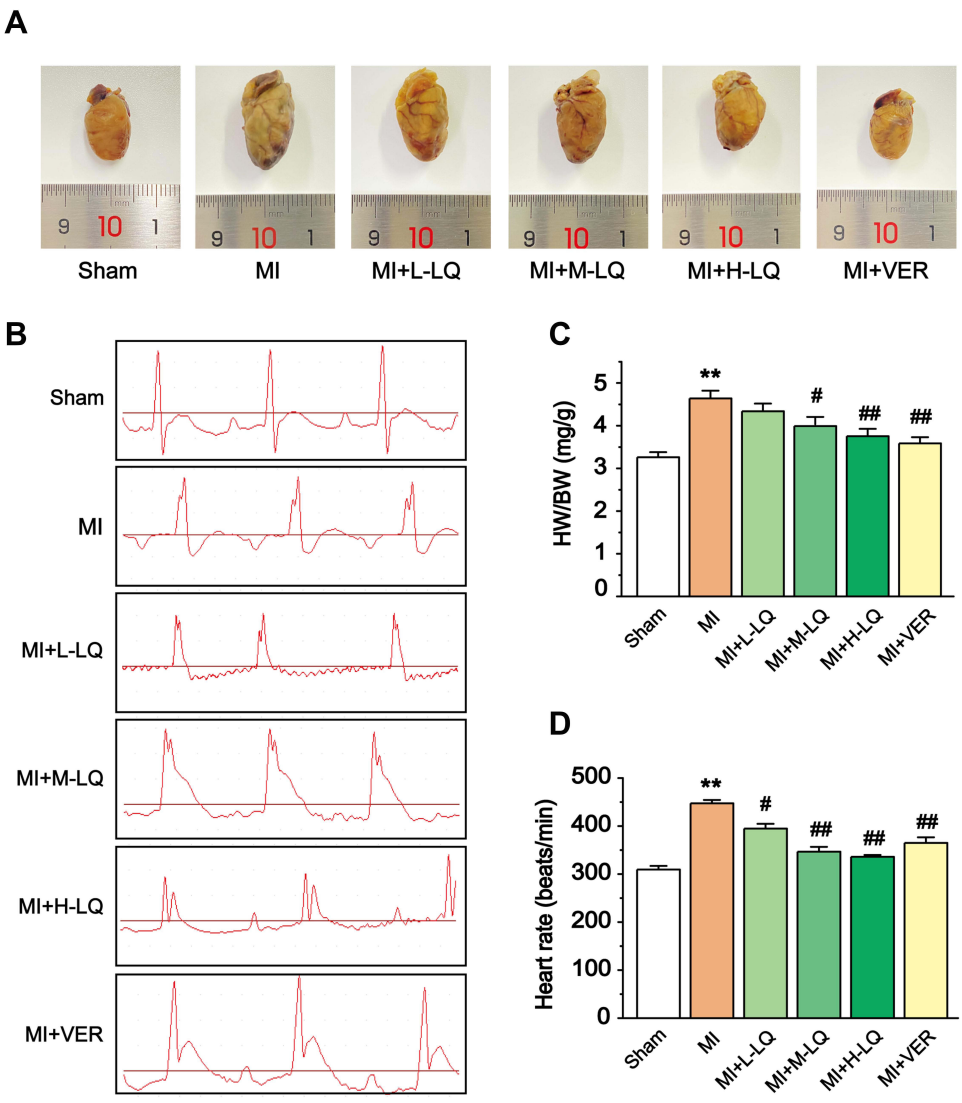

Figure 2 Effects of LQ on (**A**) gross appearances, (**B**) ECG, (**C**) HW/BW, and (**D**) heart rate of each group. Values measured are presented as the mean ± SEM (n = 5). $^{**}P < 0.01$ vs Sham group; $^{\#}P < 0.05$, $^{\#\#}P < 0.01$ vs MI group.

from the Sham groups in appearance. As shown in Figure 2B, D, the heart rate was increased in MI rats in comparison to Sham rats ($P < 0.01$). Rats treated with LQ and VER had significantly reduced heart rates compared to MI rats ($P < 0.01$ or $P < 0.05$). HW/BW was increased in MI rats compared to the Sham rats ($P < 0.01$) and was reduced in the LQ and VER groups compared to the MI group ($P < 0.01$ or $P < 0.05$) (Figure 2C).

LQ Down-Regulated Myocardial Markers

Figure 3A–E present the effects of LQ on myocardial markers of MI rats. Rats in the MI group exhibited significantly higher serum CK, LDH, CK-MB, cTnI and BNP levels in comparison to the Sham group ($P < 0.01$). Conversely, this alteration in biochemical parameters was reversed with LQ and VER ($P < 0.05$ or $P < 0.01$). The results indicate that LQ can improve MI-induced cardiac damage.

LQ Reduced Infarct Area and Improved Cardiac Function

To visualize the effect of LQ on myocardial infarct size and left ventricular failure, we performed TTC staining and hemodynamic evaluation (Figure 4). The results of TTC staining demonstrated no infarcts in the Sham group, while the

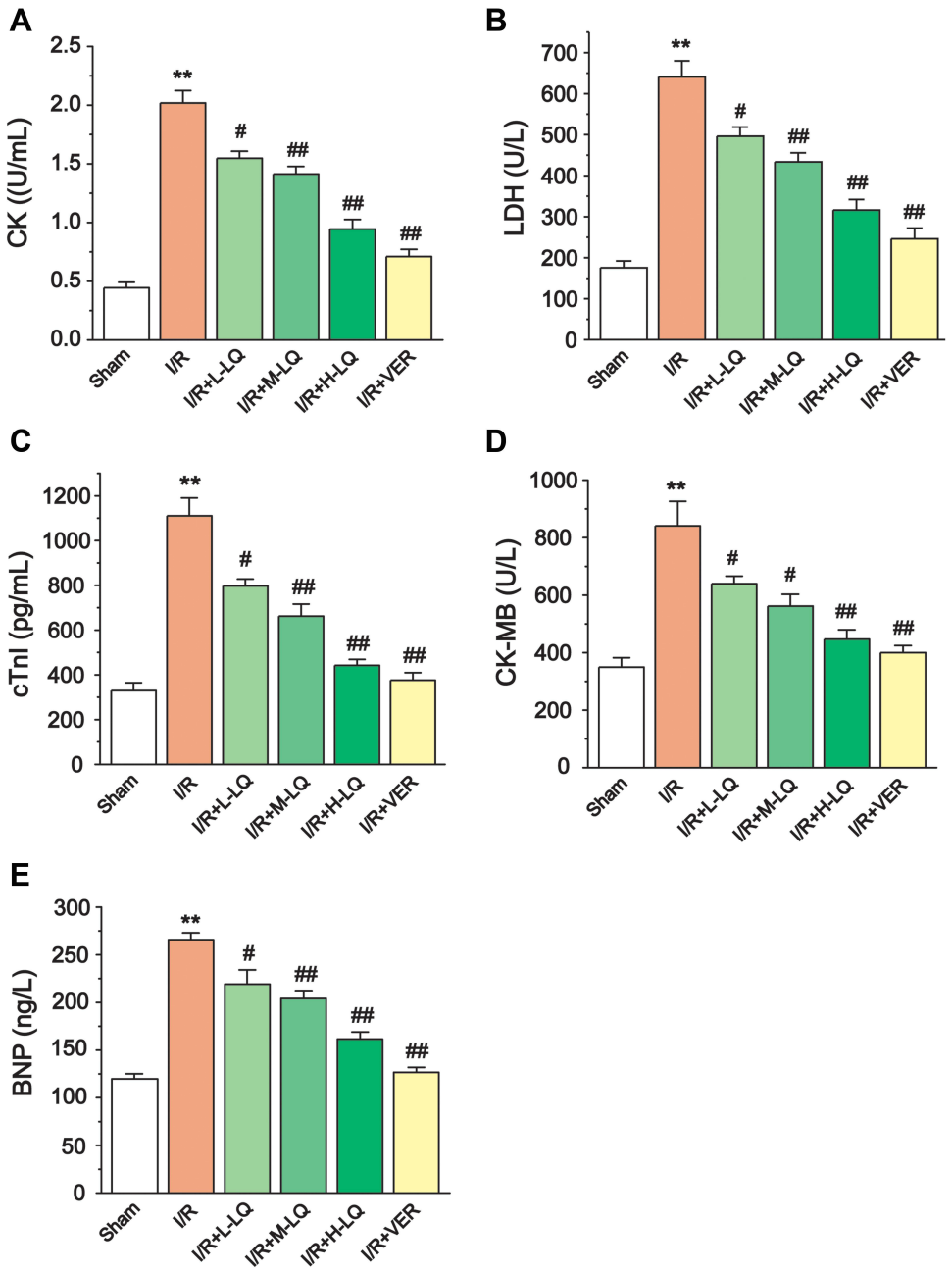

Figure 3 Effects of LQ on myocardial markers. (**A**) CK, (**B**) LDH, (**C**) cTnI, (**D**) CK-MB and (**E**) BNP. Values measured are presented as the mean ± SEM (n = 5). $^{**}P < 0.01$ vs Sham group; $^{\#}P < 0.05$, $^{\#\#}P < 0.01$ vs MI group.

infarct areas in the MI group were clearly larger than those in the Sham group ($P < 0.01$). Nevertheless, the area of MI was dramatically reduced by LQ and VER treatment ($P < 0.05$) (Figure 4A and B).

As shown in Figure 4C–E, we observed the effects of LQ on hemodynamics by comparing the levels of LVEDP, LVSP and $\pm dp/dt_{max}$ in each group of rats. Compared with the Sham group, the MI group had dramatically higher LVEDP levels and significantly lower $\pm dp/dt_{max}$ levels ($P < 0.01$). Notably, the values of hemodynamic parameters of rats were significantly restored in the LQ-treated and VER groups ($P < 0.05$ or $P < 0.01$).

LQ Improved Myocardial Morphology

As shown in Figure 5, we explored the effects of LQ on histopathological changes in rats with MI. The results of HE staining showed typical myofibrillar structure in the Sham group, while the MI group had significant swelling of

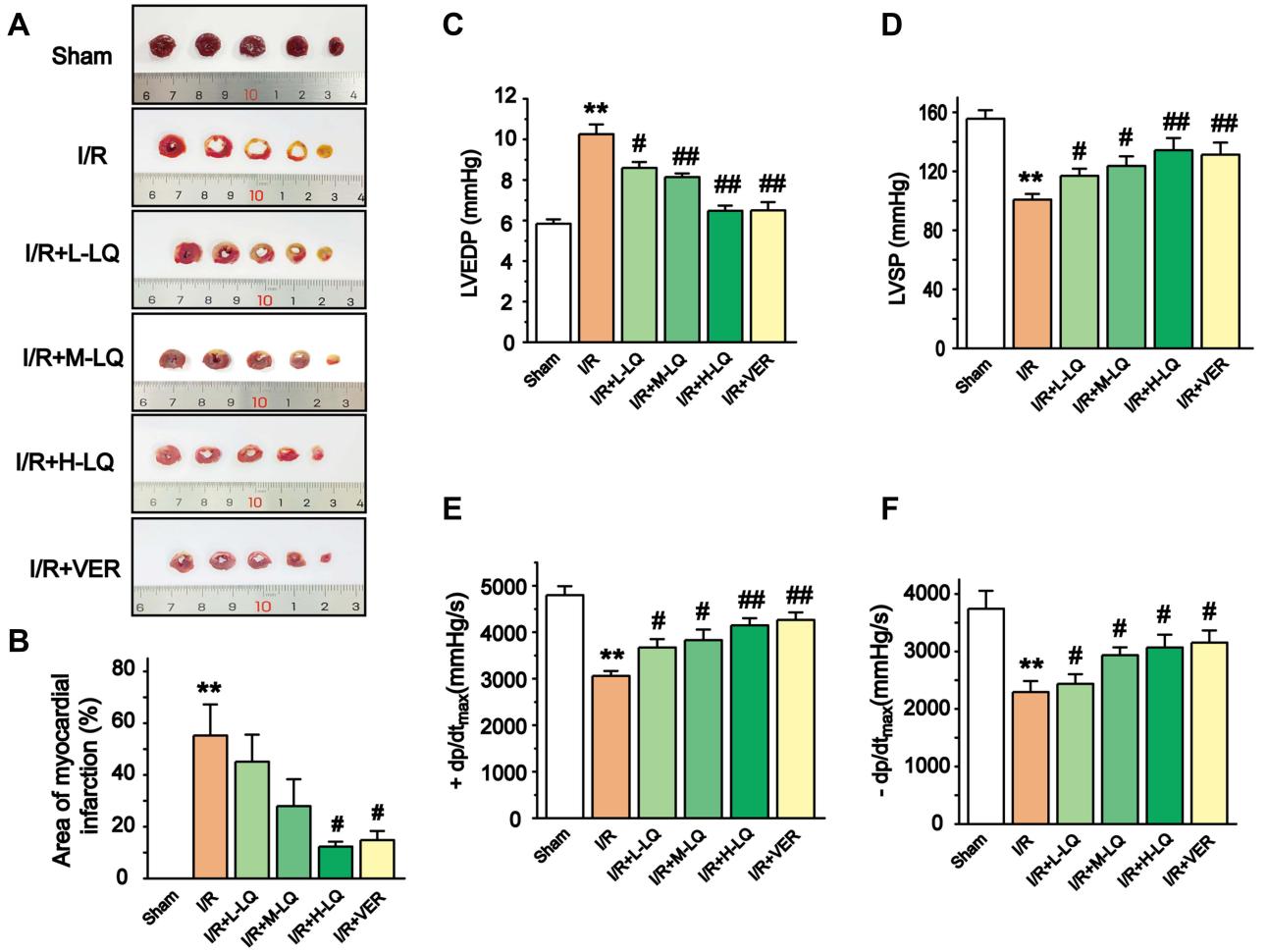

Figure 4 Effects of LQ on area of myocardial infarction and hemodynamic parameters in each group. (**A**) Representative diagram of TTC staining of heart sections. (**B**) The infarct size was assessed as the ratio of infarct area to total myocardial area. Hemodynamic parameters including (**C**) LVEDP, (**D**) LVSP, (**E**) +dP/dt_{max}, and (**F**) -dP/dt_{max}. Values measured are presented as the mean ± SEM (n = 5). $^{**}P < 0.01$ vs Sham group; $^{\#}P < 0.05$, $^{\#\#}P < 0.01$ vs MI group.

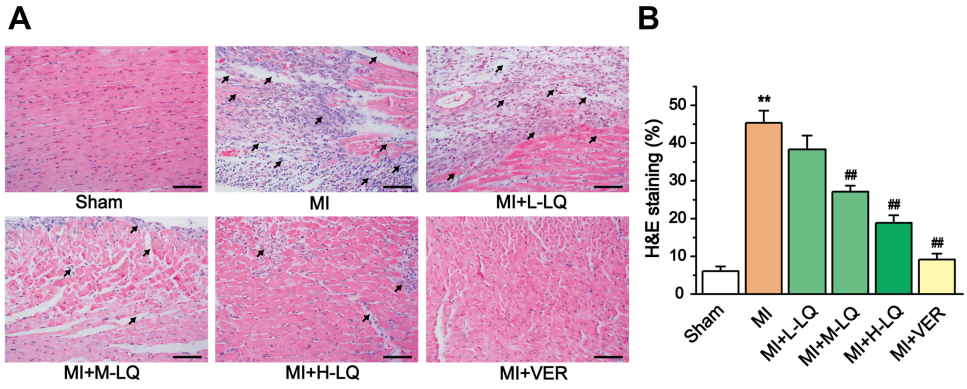

Figure 5 Effects of LQ on histopathological changes of heart observed by H&E staining (200×). (**A**) Representative images of H&E staining for each group. (**B**) The percentage of myocardial injury areas were calculated. The arrows on the image show the site of myocardial damage. Bars represent 100 μm. Values are presented as the mean ± SEM (n = 3). $^{**}P < 0.01$ vs Sham group; $^{\#\#}P < 0.01$ vs MI group.

cardiomyocytes, disorganized myofibrillar arrangement, and infiltration of inflammatory cells. Although edema and inflammatory cells were still present in the LQ group, they were to a lesser extent compared to the MI group.

Next, we observed the effects of LQ on MF. In the figure, the regions in blue between myocardial cells are collagen fibers. Figure 6 shows that there was an increase in the number of blue-stained fibers and significant MF in the MI group

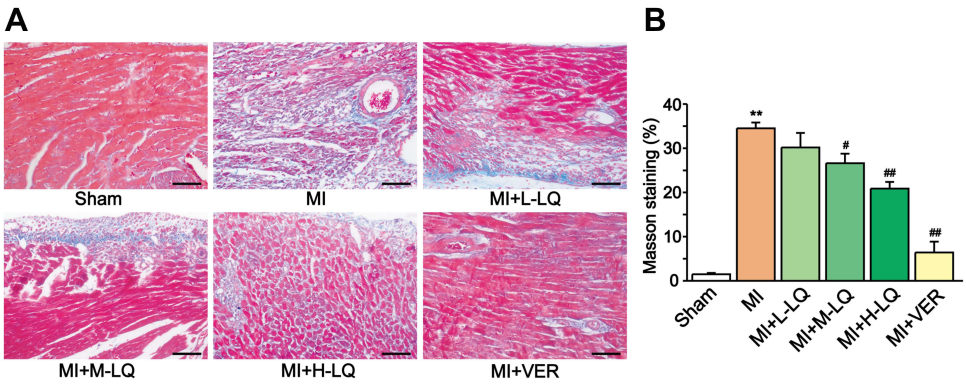

Figure 6 Effects of LQ on histopathological changes of heart observed by Masson staining (200×). (**A**) Representative images of Masson staining for each group. (**B**) The percentage of positive areas were calculated. Bars represent 100 μm. Values are presented as the mean ± SEM (n = 3). $^{**}P < 0.01$ vs Sham group; $^{\#}P < 0.05$, $^{\#\#}P < 0.01$ vs MI group.

rats. The LQ and VER groups showed improved myocardial cell disorder arrangement, reduced collagen deposition, and improved MF compared with the MI group.

LQ Inhibited the Expressions of Collagen I, Collagen III, TGF-β1, MMP-9, and α-SMA

As shown in Figure 7, Western blotting assay results indicated that protein expressions of Collagen I, Collagen III, TGF-β1, MMP-9, and α-SMA were obviously upregulated in the MI group when compared with the Sham group ($P < 0.01$). As compared to the MI group, we found that the protein expressions of Collagen I, Collagen III, TGF-β1, MMP-9, and α-SMA were remarkably reduced in both the LQ and VER groups ($P < 0.01$ or $P < 0.05$). Our results suggest that LQ could reduce MF.

LQ Inhibited Cardiac Oxidative Stress

As shown in Figure 8, the MDA levels in the MI group were markedly elevated, while SOD levels decreased significantly ($P < 0.01$). Conversely, LQ-treated and VER groups had lower MDA content and higher SOD levels compared to the MI group ($P < 0.01$ or $P < 0.05$).

LQ Down-Regulated Inflammatory Cytokines

Figure 9 illustrates the effects of LQ on inflammatory cytokine secretion according to the levels of TNF-α and IL-6. Notably, the cytokines TNF-α and IL-6, which regulate inflammatory cell chemotaxis and adhesion, were significantly increased during MI injury compared to the Sham group ($P < 0.01$). The LQ-treated and VER groups, on the other hand, showed clearly decreased levels of TNF-α and IL-6 compared to the MI group ($P < 0.01$ or $P < 0.05$).

LQ Inhibited CCL5 Expression and NF-κB Signaling Pathway

As shown in Figure 10, CCL5 and p-NF-κB were highly expressed in the MI group when compared to the Sham group ($P < 0.01$). However, the expression of CCL5 and p-NF-κB proteins in the LQ and VER groups was obviously decreased compared to those in the MI group ($P < 0.01$). Our results suggest that LQ may inhibit the inflammatory response after MI by suppressing CCL5 expression and the NF-κB pathway.

Discussion

Flavonoids are considered to be potent antioxidants with the potential to reduce cellular fibrosis or damage. Also, they have the potential to inhibit the onset and progression of inflammatory diseases.[35] Studies have demonstrated the ability of LQ to inhibit high fructose-induced MF and cardioprotective effects by reducing inflammation in various animal models.[23,36,37] Our study explored the role of LQ in MF after MI.

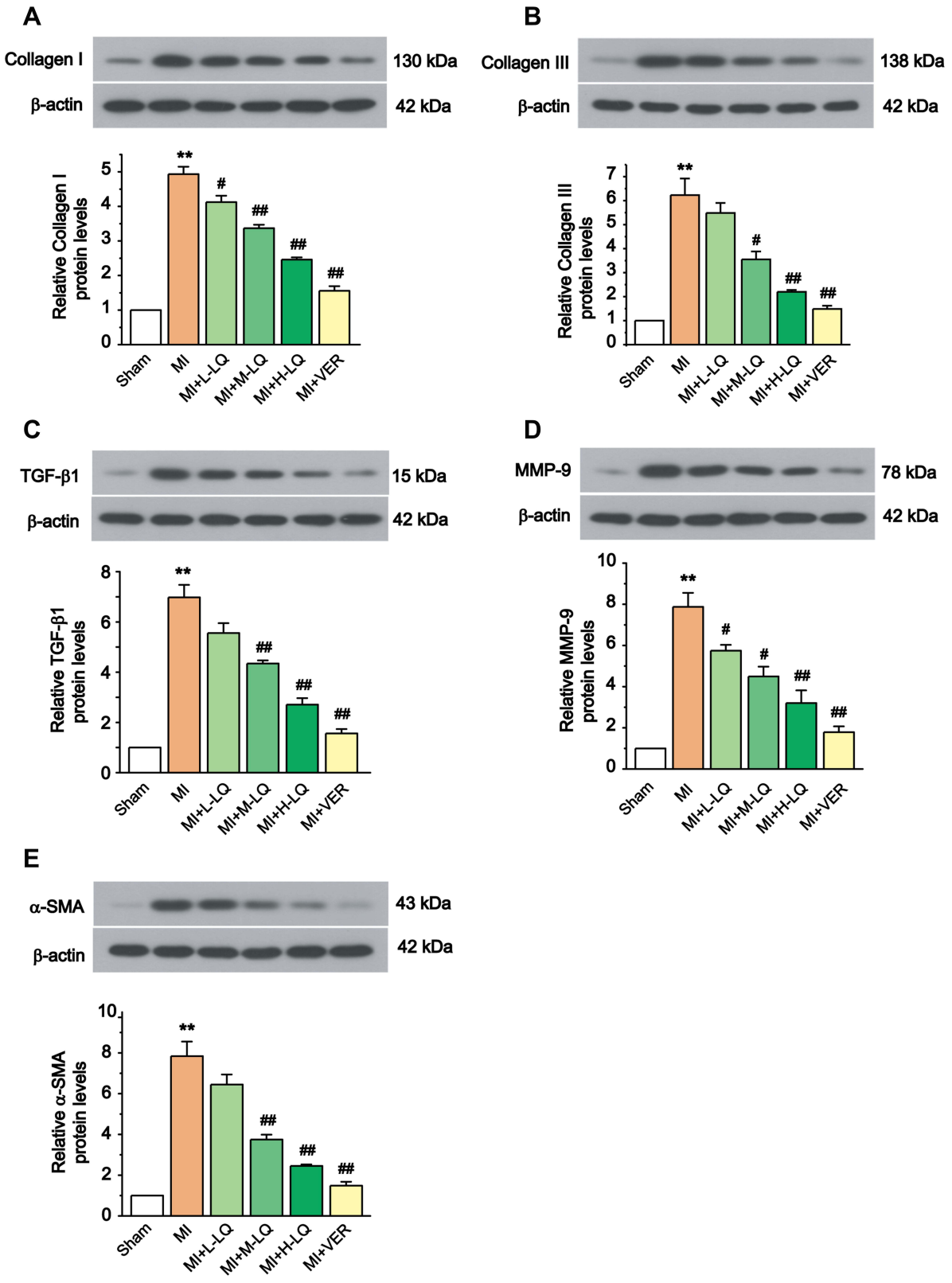

Figure 7 Effects of LQ on the protein expressions of Collagen I, Collagen III, TGF-β1, MMP-9, and α-SMA protein expressions in heart tissue. The anti-β-actin antibody was used to demonstrate that the proteins were loaded equally. Relative intensities of (**A**) Collagen I, (**B**) Collagen III, (**C**) TGF-β1, (**D**) MMP-9, and (**E**) α-SMA were calculated by normalization to the β-actin. Values measured are presented as the mean ± SEM (n = 3). $^{**}P < 0.01$ vs Sham group; $^{\#}P < 0.05$, $^{\#\#}P < 0.01$ vs MI group.

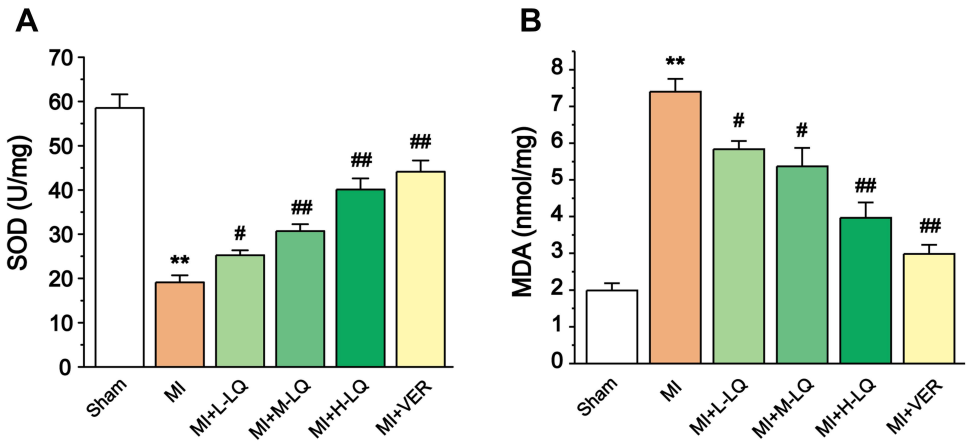

Figure 8 Effects of LQ on activities of (**A**) SOD and concentration of (**B**) MDA. Values measured are presented as the mean ± SEM (n = 5). $^{**}P < 0.01$ vs Sham group; $^{\#}P < 0.05$, $^{\#\#}P < 0.01$ vs MI group.

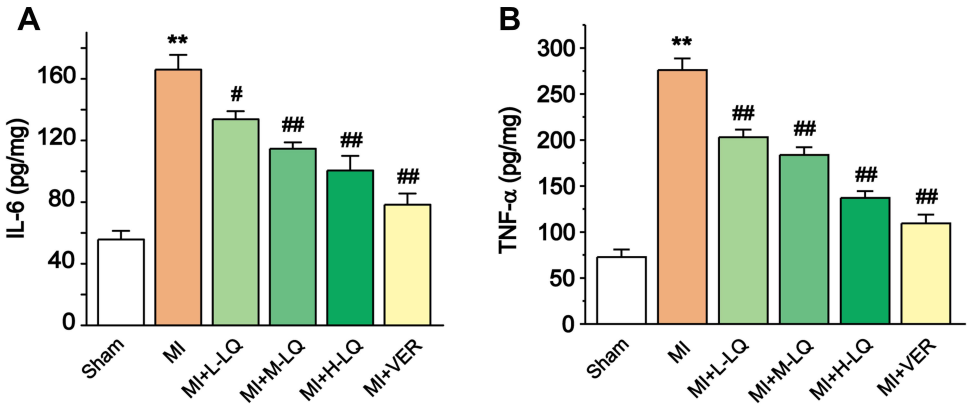

Figure 9 Effects of LQ on the concentration of (**A**) IL-6 and (**B**) TNF-α. Values measured are presented as the mean ± SEM (n = 5). $^{**}P < 0.01$ vs Sham group; $^{\#}P < 0.05$, $^{\#\#}P < 0.01$ vs MI group.

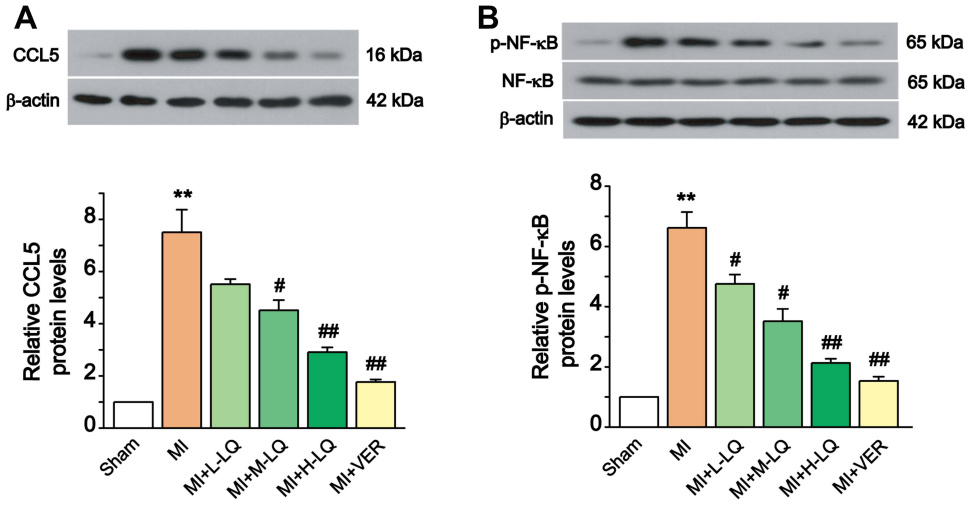

Figure 10 Effects of LQ on the protein expressions of CCL5 and NF-κB in heart tissue. The relative intensities of (**A**) CCL5, (**B**) NF-κB and p-NF-κB in each group were determined by normalizing to the β-actin. Values measured are presented as the mean ± SEM (n = 3). $^{**}P < 0.01$ vs Sham group; $^{\#}P < 0.05$, $^{\#\#}P < 0.01$ vs MI group.

Clinically, improper treatment of MI causes complications such as heart failure, ventricular remodeling, and cardiac insufficiency, which seriously endanger human health.[11,38] Adverse myocardial remodeling following MI forms the basis of ischemic heart failure, including complex short- and long-term changes in the left ventricle, cardiac shape, function, and cellular and molecular composition.[39,40]

In clinical practice, calcium antagonists are recommended by treatment guidelines as first-line therapeutic agents for stable coronary ischemic disease.[41] Verapamil (VER), as a calcium channel blocker, can be used for the prevention and relief of angina pectoris.[42,43] Also, it has been extensively studied as a positive control drug in myocardial ischemia experiments[44,45] and has shown significant anti-ischemic effects.[46,47] Therefore, VER was used as a positive control drug in this research.

In our experiment, we found that LQ significantly improved cardiac function and attenuated adverse remodeling of the heart due to excessive non-infarct zone volume and pressure. This is reflected in the ability of LQ to improve cardiac appearance, ECG, HW/BW, myocardial infarct size, and hemodynamic indices. In addition, LQ also decreased the levels of myocardial markers, such as CK, CK-MB, cTnI and LDH. The cardiovascular peptide hormone BNP is a sensitive and accurate indicator of changes in left ventricular function.[48] The MI-induced increase in BNP concentration was significantly reversed by LQ treatment. The effect of LQ on these indicators suggests that it has therapeutic effects on MI.

The mortality rate of MI has been high in recent years. Myocardial ischemia causes MF primarily due to loss of normal cardiomyocytes, formation of scar myocardium and myocardial dilatation.[49] Both interstitial and replacement fibrosis may influence the ventricular structure and systolic-diastolic function of the heart, thus contributing to the pathophysiological basis of ischemic heart failure.[40,50]

H&E staining showed that cardiomyocytes had significant swelling, disorganized myofiber arrangement, and infiltration of inflammatory cells in the MI group of rats. Furthermore, Masson staining indicated a large amount of blue collagen deposition between the myocardium after MI. Notably, LQ significantly improved these pathological changes. Our results suggest that MF after MI could be ameliorated by LQ.

Myocardial structure and function are negatively affected by excessive MF, a frequent clinical result of several heart illnesses, including MI.[51,52] Under ischemic conditions, cardiac fibroblasts transform into myofibroblasts and secrete large amounts of ECM, including collagen.[53] During this process, the expression of α-SMA in the myocardium is increased.[7] The massive deposition of ECM and the decrease in the degradation of ECM lead to an imbalance and disturbance of the collagen structure, which eventually leads to MF.[11] The imbalance of MMP and excessive secretion of cytokines such as TGF-β eventually leads to MF.[54,55] It has been shown that the upregulation of MMPs after MI leads to a reduction in myocardial tissue thickness (thinning of the ventricular wall), which ultimately leads to deterioration of cardiac function.[8,56] Yan et al found that MMP-9 expression was increased after MF and was involved in myocardial remodeling after MI.[57] Also, diffuse accumulation of Collagen I and Collagen III in the intercellular matrix causes MF.[58]

The results of the Western blotting demonstrated that the expressions of Collagen I and Collagen III were remarkably increased in the MI group rats, accompanied by increased levels of SMA-α, MMP-9 and TGF-β. However, LQ significantly suppressed the levels of these MF-related biomarkers. Our results show that LQ plays a major role in the anti-MF process.

After MI, the increase in oxidation levels in myocardial tissue is positively correlated with the degree of myocardial injury.[49] Our experimental results indicate that LQ increases the activity of SOD and decreases the level of MDA, reducing the damage during MI. Furthermore, the inflammatory response after MI is another factor that affects cardiac function and remodeling. It is known that the inflammatory response can further aggravate cardiac remodeling and myocardial injury.[12] We found that LQ reduced the levels of IL-6 and TNF-α. Increased expression of inflammatory factors promotes the proliferation of resting fibroblasts and their conversion into myofibroblasts, increasing collagen deposition and leading to MF.[59]

Persistent inflammation can aggravate detrimental remodeling of the heart and cause MI even though inflammation is necessary to repair damaged tissue and encourage recovery.[60] Therefore, MI is closely related to inflammation and

fibrosis. Identifying key factors that improve the induction of MI is critical to the targeted development of novel therapeutic agents against MI. Studies have reported that myocardial reperfusion injury increases CCL5 expression and that CCL5 antagonist treatment decreases the myocardial infarct size and cytokine secretion.[14] CCL5 has been identified as a key regulator of early fibrotic events in the development of nonalcoholic fatty liver disease.[61,62] We found that the protective effect of LQ against MI was associated with the inhibition of CCL5 expression.

NF-κB is a central transcriptional effector of inflammatory signaling and can be activated by CCL5 binding to its ligand. After MI, activation of NF-κB and its subsequent nuclear translocation trigger a plethora of inflammatory cytokines, chemokines, and adhesion molecules. The expression of these mediators further amplifies the inflammatory response and attracts and recruits specific leukocyte populations to the damaged myocardium.[18] In this study, LQ significantly inhibited the expression of p-NF-κB. Our results suggest that LQ attenuates the myocardial fibrotic response after MI, which possibly occurs by inhibiting the nuclear translocation of NF-κB.

Conclusion

Our results demonstrated that LQ improved cardiac function, reduced myocardial infarct size, attenuated pathological damage of the heart, suppressed oxidative stress and inflammatory responses, and decreased the expression of MF-related biomarkers. Furthermore, we found that LQ attenuated MF after MI, possibly by inhibiting CCL5 expression and the NF-κB pathway (Figure 11). Our study reveals a potential link between LQ and the pathogenesis of MI and provides an experimental basis for LQ in treatment.

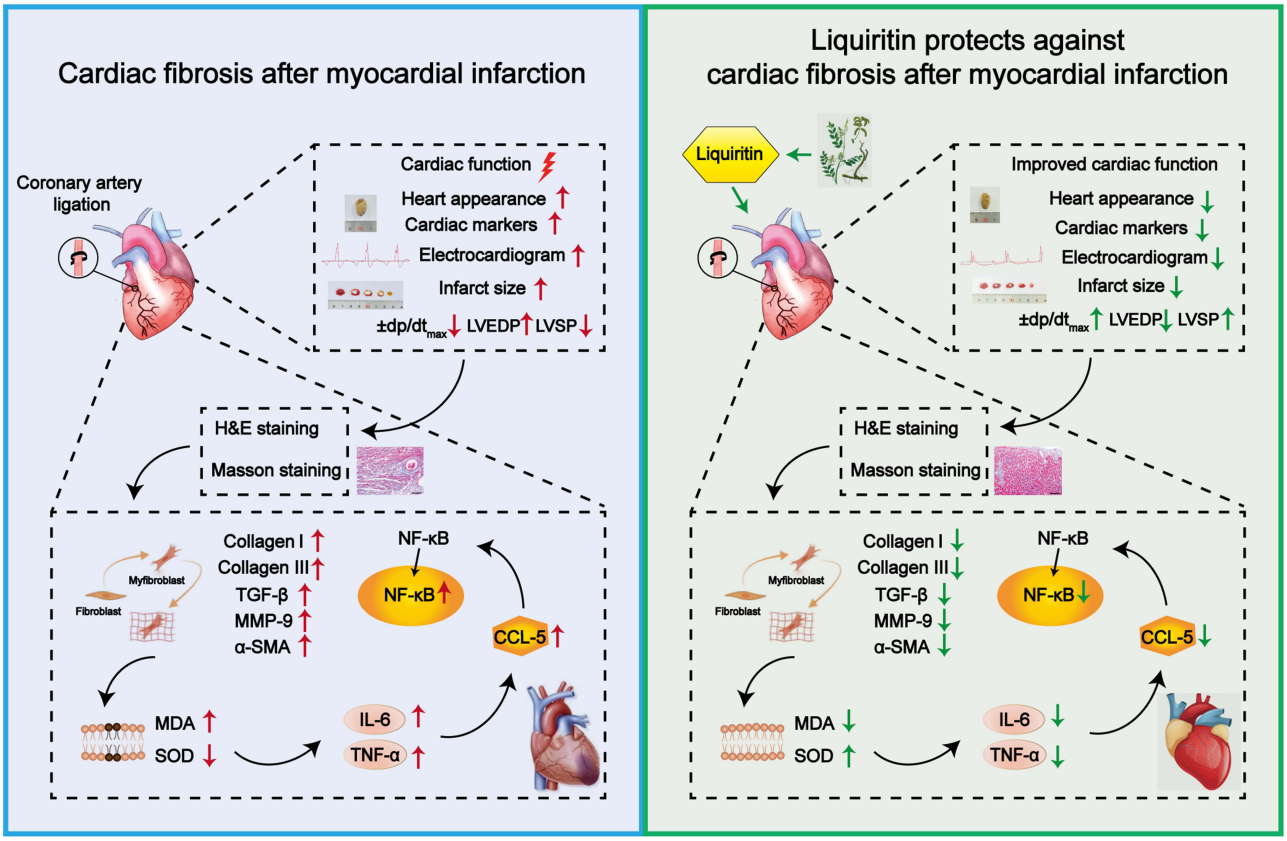

Figure 11 Schematic diagram of the protective effects of LQ on myocardial infarction damage.

Acknowledgments

This work was supported by the Research Foundation of Natural Science of Hebei Province Youth Project (No. H2021423027) and Construction Program of New Research and Development Platform and Institution, Hebei Province Innovation Ability Promotion Plan (No. 20567624H).

Disclosure

The authors report no conflicts of interest in this work.

References

1. Hausenloy DJ, Yellon DM. Myocardial ischemia-reperfusion injury: a neglected therapeutic target. *J Clin Invest*. 2013;123(1):92–100. doi:10.1172/JCI62874
2. Kuruvilla S, Adenaw N, Katwal AB, Lipinski MJ, Kramer CM, Salerno M. Late gadolinium enhancement on cardiac magnetic resonance predicts adverse cardiovascular outcomes in nonischemic cardiomyopathy: a systematic review and meta-analysis. *Circ Cardiovasc Imaging*. 2014;7(2):250–258. doi:10.1161/CIRCIMAGING.113.001144
3. Espeland T, Lunde IG, Gullestad L, Aakhus S. Myocardial fibrosis. *Tidsskr nor Laegeforen*. 2018;138:16.
4. Scalise RFM, De Sarro R, Caracciolo A, et al. Fibrosis after myocardial infarction: an overview on cellular processes, molecular pathways, clinical evaluation and prognostic value. *Med Sci*. 2021;9:1.
5. Xue K, Zhang J, Li C, et al. The role and mechanism of transforming growth factor beta 3 in human myocardial infarction-induced myocardial fibrosis. *J Cell Mol Med*. 2019;23(6):4229–4243. doi:10.1111/jcmm.14313
6. Polyakova V, Loeffler I, Hein S, et al. Fibrosis in endstage human heart failure: severe changes in collagen metabolism and MMP/TIMP profiles. *Int J Cardiol*. 2011;151(1):18–33. doi:10.1016/j.ijcard.2010.04.053
7. Fu X, Khalil H, Kanisicak O, et al. Specialized fibroblast differentiated states underlie scar formation in the infarcted mouse heart. *J Clin Invest*. 2018;128(5):2127–2143. doi:10.1172/JCI98215
8. Spinale FG. Myocardial matrix remodeling and the matrix metalloproteinases: influence on cardiac form and function. *Physiol Rev*. 2007;87(4):1285–1342. doi:10.1152/physrev.00012.2007
9. Liu M, Li W, Wang H, et al. CTRP9 Ameliorates atrial inflammation, fibrosis, and vulnerability to atrial fibrillation in post-myocardial infarction rats. *J Am Heart Assoc*. 2019;8(21):e013133. doi:10.1161/JAHA.119.013133
10. Rajesh M, Mukhopadhyay P, Batkai S, et al. Cannabidiol attenuates cardiac dysfunction, oxidative stress, fibrosis, and inflammatory and cell death signaling pathways in diabetic cardiomyopathy. *J Am Coll Cardiol*. 2010;56(25):2115–2125. doi:10.1016/j.jacc.2010.07.033
11. Dufeys C, Daskalopoulos EP, Castanares-Zapatero D, et al. AMPKα1 deletion in myofibroblasts exacerbates post-myocardial infarction fibrosis by a connexin 43 mechanism. *Basic Res Cardiol*. 2021;116(1):10. doi:10.1007/s00395-021-00846-y
12. Toldo S, Abbate A. The NLRP3 inflammasome in acute myocardial infarction. *Nat Rev Cardiol*. 2018;15(4):203–214. doi:10.1038/nrcardio.2017.161
13. Kraaijeveld AO, de Jager SC, de Jager WJ, et al. CC chemokine ligand-5 (CCL5/RANTES) and CC chemokine ligand-18 (CCL18/PARC) are specific markers of refractory unstable angina pectoris and are transiently raised during severe ischemic symptoms. *Circulation*. 2007;116(17):1931–1941. doi:10.1161/CIRCULATIONAHA.107.706986
14. Braunersreuther V, Pellieux C, Pelli G, et al. Chemokine CCL5/RANTES inhibition reduces myocardial reperfusion injury in atherosclerotic mice. *J Mol Cell Cardiol*. 2010;48(4):789–798. doi:10.1016/j.yjmcc.2009.07.029
15. Li M, Sun X, Zhao J, et al. CCL5 deficiency promotes liver repair by improving inflammation resolution and liver regeneration through M2 macrophage polarization. *Cell Mol Immunol*. 2020;17(7):753–764. doi:10.1038/s41423-019-0279-0
16. Long H, Xie R, Xiang T, et al. Autocrine CCL5 signaling promotes invasion and migration of CD133+ ovarian cancer stem-like cells via NF-κB-mediated MMP-9 upregulation. *Stem Cells*. 2012;30(10):2309–2319. doi:10.1002/stem.1194
17. Lawrence T. The nuclear factor NF-kappaB pathway in inflammation. *Cold Spring Harb Perspect Biol*. 2009;1(6):a001651. doi:10.1101/cshperspect.a001651
18. Prabhu SD, Frangogiannis NG. The biological basis for cardiac repair after myocardial infarction: from inflammation to fibrosis. *Circ Res*. 2016;119(1):91–112. doi:10.1161/CIRCRESAHA.116.303577
19. Jiang M, Zhao S, Yang S, et al. An "essential herbal medicine"-licorice: a review of phytochemicals and its effects in combination preparations. *J Ethnopharmacol*. 2020;249:112439. doi:10.1016/j.jep.2019.112439
20. Qin J, Chen J, Peng F, et al. Pharmacological activities and pharmacokinetics of liquiritin: a review. *J Ethnopharmacol*. 2022;293:115257. doi:10.1016/j.jep.2022.115257
21. Tang TJ, Wang X, Wang L, et al. Liquiritin inhibits H2O2-induced oxidative stress injury in H9c2 cells via the AMPK/SIRT1/NF-κB signaling pathway. *J Food Biochem*. 2022;46(10):e14351. doi:10.1111/jfbc.14351
22. Aiyasiding X, Liao HH, Feng H, et al. Liquiritin attenuates pathological cardiac hypertrophy by activating the PKA/LKB1/AMPK pathway. *Front Pharmacol*. 2022;13:870699. doi:10.3389/fphar.2022.870699
23. Mou SQ, Zhou ZY, Feng H, et al. Liquiritin attenuates lipopolysaccharides-induced cardiomyocyte injury via an AMP-activated protein kinase-dependent signaling pathway. *Front Pharmacol*. 2021;12:648688. doi:10.3389/fphar.2021.648688
24. Sun J, Wugeti N, Mahemuti A. Reversal effect of Zhigancao decoction on myocardial fibrosis in a rapid pacing-induced atrial fibrillation model in New Zealand rabbits. *J Int Med Res*. 2019;47(2):884–892. doi:10.1177/0300060518799819
25. Shi X, Zhu H, Zhang Y, Zhou M, Tang D, Zhang H. XuefuZhuyu decoction protected cardiomyocytes against hypoxia/reoxygenation injury by inhibiting autophagy. *BMC Complement Altern Med*. 2017;17(1):325. doi:10.1186/s12906-017-1822-0
26. Liu M, Xue Y, Liang Y, et al. Mechanisms underlying the cardioprotection of YangXinDingJi Capsule against myocardial Ischemia in rats. *Evid Based Complement Alternat Med*. 2020;2020:8539148. doi:10.1155/2020/8539148

27. Cheng S, Zhang X, Feng Q, et al. Astragaloside IV exerts angiogenesis and cardioprotection after myocardial infarction via regulating PTEN/PI3K/Akt signaling pathway. *Life Sci*. 2019;227:82–93. doi:10.1016/j.lfs.2019.04.040
28. Wang Q, Liu AD, Li TS, Tang Q, Wang XC, Chen XB. Ghrelin ameliorates cardiac fibrosis after myocardial infarction by regulating the Nrf2/NADPH/ROS pathway. *Peptides*. 2021;144:170613. doi:10.1016/j.peptides.2021.170613
29. Zhang HR, Bai H, Yang E, et al. Effect of moxibustion preconditioning on autophagy-related proteins in rats with myocardial ischemia reperfusion injury. *Ann Transl Med*. 2019;7(20):559. doi:10.21037/atm.2019.09.66
30. Huang Z, Zhao Q, Chen M, Zhang J, Ji L. Liquiritigenin and liquiritin alleviated monocrotaline-induced hepatic sinusoidal obstruction syndrome via inhibiting HSP60-induced inflammatory injury. *Toxicology*. 2019;428:152307. doi:10.1016/j.tox.2019.152307
31. Li Y, Xia C, Yao G, et al. Protective effects of liquiritin on UVB-induced skin damage in SD rats. *Int Immunopharmacol*. 2021;97:107614. doi:10.1016/j.intimp.2021.107614
32. Huang X, Wang Y, Ren K. Protective Effects of liquiritin on the brain of rats with Alzheimer's disease. *West Indian Med J*. 2015;64(5):468–472. doi:10.7727/wimj.2016.058
33. Xue Y, Li M, Xue Y, et al. Mechanisms underlying the protective effect of tannic acid against arsenic trioxide induced cardiotoxicity in rats: potential involvement of mitochondrial apoptosis. *Mol Med Rep*. 2020;22(6):4663–4674. doi:10.3892/mmr.2020.11586
34. Wang H, Jiang C, Yang Y, et al. Resveratrol ameliorates iron overload induced liver fibrosis in mice by regulating iron homeostasis. *PeerJ*. 2022;10:e13592. doi:10.7717/peerj.13592
35. Maleki SJ, Crespo JF, Cabanillas B. Anti-inflammatory effects of flavonoids. *Food Chem*. 2019;299:125124. doi:10.1016/j.foodchem.2019.125124
36. Zhang Y, Zhang L, Zhang Y, Xu JJ, Sun LL, Li SZ. The protective role of liquiritin in high fructose-induced myocardial fibrosis via inhibiting NF-κB and MAPK signaling pathway. *Biomed Pharmacother*. 2016;84:1337–1349. doi:10.1016/j.biopha.2016.10.036
37. Zhang X, Song Y, Han X, et al. Liquiritin attenuates advanced glycation end products-induced endothelial dysfunction via RAGE/NF-κB pathway in human umbilical vein endothelial cells. *Mol Cell Biochem*. 2013;374(1–2):191–201. doi:10.1007/s11010-012-1519-0
38. Bajpai G, Bredemeyer A, Li W, et al. Tissue resident CCR2- and CCR2+ cardiac macrophages differentially orchestrate monocyte recruitment and fate specification following myocardial injury. *Circ Res*. 2019;124(2):263–278. doi:10.1161/CIRCRESAHA.118.314028
39. Bhatt AS, Ambrosy AP, Velazquez EJ. Adverse remodeling and reverse remodeling after myocardial infarction. *Curr Cardiol Rep*. 2017;19(8):71. doi:10.1007/s11886-017-0876-4
40. Prabhu SD. Post-infarction ventricular remodeling: an array of molecular events. *J Mol Cell Cardiol*. 2005;38(4):547–550. doi:10.1016/j.yjmcc.2005.01.014
41. Pascual I, Moris C, Avanzas P. Beta-blockers and calcium channel blockers: first line agents. *Cardiovasc Drugs Ther*. 2016;30(4):357–365. doi:10.1007/s10557-016-6682-1
42. Kelly DT. Verapamil in angina pectoris. *Br J Clin Pharmacol*. 1986;21:191S–195S. doi:10.1111/j.1365-2125.1986.tb02870.x
43. Forslund L, Hjemdahl P, Held C, et al. Prognostic implications of results from exercise testing in patients with chronic stable angina pectoris treated with metoprolol or verapamil. A report from the Angina Prognosis Study In Stockholm (APSIS). *Eur Heart J*. 2000;21(11):901–910. doi:10.1053/euhj.1999.1936
44. Zhang K, Bai Y, Song T, Zhang G. In vivo and in vitro evidence of protective effects of a natural flavone on rat myocardial ischemia-reperfusion and hypoxia-reoxygenation injuries. *J Cardiovasc Pharmacol Ther*. 2013;18(1):31–36. doi:10.1177/1074248412461713
45. Gatsura SV. Oxygen-dependent mechanisms underlying the antiischemic effect of verapamil and amlodipine. *Bull Exp Biol Med*. 2004;137(1):40–42. doi:10.1023/B:BEBM.0000024382.81356.04
46. Blidaru M, Cuparencu B, Plesca-Manea L. The influence of intracerebroventricular administration of (±) propranolol and (±) verapamil on experimental myocardial ischemia and necrosis in rats. *Acta Physiol Hung*. 2000;87(1):99–111. doi:10.1556/APhysiol.87.2000.1.11
47. Liu P, Li J, Liu M, et al. Hesperetin modulates the Sirt1/Nrf2 signaling pathway in counteracting myocardial ischemia through suppression of oxidative stress, inflammation, and apoptosis. *Biomed Pharmacother*. 2021;139:111552. doi:10.1016/j.biopha.2021.111552
48. Han BJ, Cao GY, Jia LY, et al. Cardioprotective effects of tetrahydropalmatine on acute myocardial infarction in rats. *Am J Chin Med*. 2022;1–18. doi:10.1142/S0192415X2250080X
49. Xie S, Deng W, Chen J, et al. Andrographolide protects against adverse cardiac remodeling after myocardial infarction through enhancing Nrf2 signaling pathway. *Int J Biol Sci*. 2020;16(1):12–26. doi:10.7150/ijbs.37269
50. Sutton MG, Sharpe N. Left ventricular remodeling after myocardial infarction: pathophysiology and therapy. *Circulation*. 2000;101(25):2981–2988. doi:10.1161/01.CIR.101.25.2981
51. Burchfield JS, Xie M, Hill JA. Pathological ventricular remodeling: mechanisms: part 1 of 2. *Circulation*. 2013;128(4):388–400. doi:10.1161/CIRCULATIONAHA.113.001878
52. Azevedo PS, Polegato BF, Minicucci MF, Paiva SA, Zornoff LA. Cardiac remodeling: concepts, clinical impact, pathophysiological mechanisms and pharmacologic treatment. *Arq Bras Cardiol*. 2016;106(1):62–69. doi:10.5935/abc.20160005
53. Humeres C, Frangogiannis NG. Fibroblasts in the Infarcted, remodeling, and failing heart. *JACC Basic Transl Sci*. 2019;4(3):449–467. doi:10.1016/j.jacbts.2019.02.006
54. Khalil H, Kanisicak O, Prasad V, et al. Fibroblast-specific TGF-β-Smad2/3 signaling underlies cardiac fibrosis. *J Clin Invest*. 2017;127(10):3770–3783. doi:10.1172/JCI94753
55. Abbate A, Salloum FN, Vecile E, et al. Anakinra, a recombinant human interleukin-1 receptor antagonist, inhibits apoptosis in experimental acute myocardial infarction. *Circulation*. 2008;117(20):2670–2683. doi:10.1161/CIRCULATIONAHA.107.740233
56. DeCoux A, Lindsey ML, Villarreal F, Garcia RA, Schulz R. Myocardial matrix metalloproteinase-2: inside out and upside down. *J Mol Cell Cardiol*. 2014;77:64–72. doi:10.1016/j.yjmcc.2014.09.016
57. Yan LL, Wei XH, Shi QP, et al. Cardiotonic Pills(R) protects from myocardial fibrosis caused by in stent restenosis in miniature pigs. *Phytomedicine*. 2022;106:154405. doi:10.1016/j.phymed.2022.154405
58. Gonzalez A, Schelbert EB, Diez J, Butler J. Myocardial interstitial fibrosis in heart failure: biological and translational perspectives. *J Am Coll Cardiol*. 2018;71(15):1696–1706. doi:10.1016/j.jacc.2018.02.021
59. Gao R, Shi H, Chang S, et al. The selective NLRP3-inflammasome inhibitor MCC950 reduces myocardial fibrosis and improves cardiac remodeling in a mouse model of myocardial infarction. *Int Immunopharmacol*. 2019;74:105575. doi:10.1016/j.intimp.2019.04.022

60. Hsu WT, Tseng YH, Jui HY, Kuo CC, Wu KK, Lee CM. 5-Methoxytryptophan attenuates postinfarct cardiac injury by controlling oxidative stress and immune activation. *J Mol Cell Cardiol*. 2021;158:101–114. doi:10.1016/j.yjmcc.2021.05.014
61. Berres ML, Koenen RR, Rueland A, et al. Antagonism of the chemokine Ccl5 ameliorates experimental liver fibrosis in mice. *J Clin Invest*. 2010;120(11):4129–4140. doi:10.1172/JCI41732
62. Li BH, He FP, Yang X, Chen YW, Fan JG. Steatosis induced CCL5 contributes to early-stage liver fibrosis in nonalcoholic fatty liver disease progress. *Transl Res*. 2017;180(103–117):e4. doi:10.1016/j.trsl.2016.08.006